

In-situ temperature, grid curvature, erosion, beam and plasma characterization of a gridded ion thruster RIT-22

IEPC-2009-160

*Presented at the 31st International Electric Propulsion Conference,
University of Michigan • Ann Arbor, Michigan • USA
September 20 – 24, 2009*

C. Bundesmann¹, M. Tartz², F. Scholze³ and H. Neumann⁴
Leibniz-Institute of Surface Modification, Leipzig, 04318, Germany

H.J. Leiter⁵
Astrium Space Transportation, Moeckmuehl, 74215, Germany

F. Scortecci⁶
Aerospazio Tecnologie s.r.l., Rapolano Terme, 53040, Italy

D. Feili⁷
Justig-Liebig-Universität Giessen, Giessen, 35392, Germany

and

P.-E. Frigot⁸ and J. Gonzalez del Amo⁹
ESA/ESTEC, 2200 AG Noordwijk, The Netherlands

Abstract: We report on the in-situ characterization of temperature, grid curvature, grid erosion, beam parameters and plasma parameters of a gridded ion thruster. The characterization is performed with a diagnostic system which consists of high-accuracy, UHV-specified 5-axis position system and five different characterization tools: a pyrometer (temperature measurements), a triangular laser head (surface profile scans), a telemicroscopy system (images), a Faraday probe (current density profile maps), and an energy-selective mass spectrometer (beam composition measurements, energy and mass scans). The test object is a gridded ion thruster RIT-22 (Astrium EADS). It is operated at different power levels ranging from 1.25 kW (1250 V/1000 mA) up to 4 kW (2000 V/2000 mA). The tests are performed in the large vacuum test facility at Aerospazio (length 11.5 m, diameter 3.8 m, volume 120 m³) and in the Jumbo facility at JLU Giessen (length 6 m, diameter 2.6 m, volume 30 m³). Here selected results are presented, which demonstrate the high capabilities of both the diagnostic system and the thruster.

¹ Senior scientist, Department of Ion Beam Technology, carsten.bundesmann@iom-leipzig.de.

² Senior scientist, Department of Ion Beam Technology, michael.tartz@iom-leipzig.de.

³ Senior scientist, Department of Ion Beam Technology, frank.scholze@iom-leipzig.de.

⁴ Senior scientist and group leader, Department of Ion Beam Technology, horst.neumann@iom-leipzig.de.

⁵ Development Electric Propulsion, TP 41, hans.leiter@astrium.eads.net.

⁶ CEO, Aerospazio, aerospazio@aerospazio.com.

⁷ Senior scientist, 1st Institute of Physics, Davar.Feili@exp1.physik.uni-giessen.de.

⁸ Electric Propulsion Engineer, ESA/ESTEC, PierreEtienne.Frigot@esa.int.

⁹ Head of Electric Propulsion Section, ESA/ESTEC, Jose.Gonzalez.del.Amo@esa.int.

Nomenclature

d	=	distance measured by the triangular laser head relative to the mean working distance of 150 mm
E_{ion}^*	=	ion energy divided by the charge number
M^*	=	ion mass divided by the charge number
R_{grid}	=	grid curvature
T_{pyr}	=	temperature measured by the pyrometer
T_{grid}	=	grid temperature
x	=	position of the linear table in x direction
y	=	position of the linear table in y direction
z	=	position of the linear table in z direction

I. Introduction

Design and development as well as qualification and acceptance of space propulsion components is always associated with extensive test programs. In contrast to the highly standardized environmental tests (vibration and shock) there are a number of distinct test methods for electric thrusters depending on their individual design. Diagnostics have evolved over the years and are very often optimized for a specific thruster concept. In the majority of cases tests are performed in a vacuum chamber with an engine in operation and others are conducted outside the chamber. Sometimes it is also necessary to open the vacuum facility during a sequence of tests in order to modify and rearrange the test setup.

An interruption of the vacuum conditions is not desired. The transition from normal pressure to high vacuum conditions and vice versa is always time consuming and related with additional costs. When the hardware test setup is to be changed there is also the risk of damaging the thruster, especially when it has to be de- then re-installed in the test facility.

The new concept of a universal electric propulsion test bench presented here eliminates these disadvantages. The test bench is equipped with several instruments for different tasks. The special arrangement provides 5 degrees of freedom (3 axis of translation, x,y,z and 2 axis of rotation) for the relative positioning of thruster and instruments. The instrumentation covers a broad range of tasks: Beam profile analysis, high resolution thermography, (grid) erosion measurement, high resolution imaging, measurement of object dimensions (e.g. grid curvature), beam composition and even direct access to the plasma potential. The user can select between the instruments and it is not necessary to open the vacuum chamber when a new selection is made.

The test bench is not specially designed for a dedicated vacuum chamber. It can be used in all vacuum test facilities which provides the minimum required dimensions.

The results described here are obtained with Astrium's high power gridded ion thruster RIT-22. However the system is not limited to gridded ion engines: tests with a Hall Effect Engine ("SPT"/ "HET) have also performed successfully using the same test setup.

II. Test Setup

A. The Diagnostic System

The diagnostic system [1,2] utilizes a UHV-specified five axis positioning system, which allows to move the diagnostic heads and the thruster or vice versa very precisely relative to each other. The positioning utilizes three linear tables with a total travelling length of 700 mm each and two rotary tables, which perform full circle rotations. The positioning accuracy of the linear tables is better than 0.1 mm and of the rotation tables better than 0.5°. The travelling speed of the linear tables is typically 30 mm/s. Travelling speeds up to 50 mm/s are successfully tested. The rotation tables are operated typically with 1 deg/s. All tables are driven by UHV-specified stepper motors and are mounted on a modular bar setup, which allows to adapt the system to the specific requirements of the vacuum chamber and the thruster. The operation of the linear and rotation tables and of the diagnostic heads is computer controlled,

For the measurements reported here, the diagnostic system is equipped with the following diagnostic tools:

- A **triangular laser head** (TLH) for measuring surface profile scans, which is used to study the grid shape changes, i.e. radius of curvature, during operation.
- A **telemicroscopy system** (TMS), which allows taking spatially resolved images of selected thruster parts, here especially of the grid holes in order to study changes of their shape or diameter.
- A **pyrometer** for temperature scans across the diameter of the outer (accelerator) grid.

- A **Faraday probe** for measuring 2D current density profile maps at selected distances up to a maximum distance of 600 mm from the thruster.
- An **energy-selective mass spectrometer (ESMS)** for studying the composition, the energy distribution and the fraction of multiple-charged ions in the thruster beam. The measurements are done in dependence on position and emission angle.

In Figure 1 the experimental setup mounted in the LVTF at Aerospazio is shown. The TLH and the pyrometer are placed inside a vacuum-sealed housing with a graphite protection shield. The housing is connected to the chamber wall by flexible tubes with KF sealing, i.e. inside the vacuum housing is normal pressure. This also avoids additional contacts for electrical feed-through. The view ports in the housing are covered by shutters, which can be opened by appropriate mechanism. The TMS is also placed in a vacuum-sealed housing with flexible tubes and a shutter made of graphite. The ESMS is mounted to the chamber, such that the thruster is to be rotated by 90 deg for ESMS measurements.

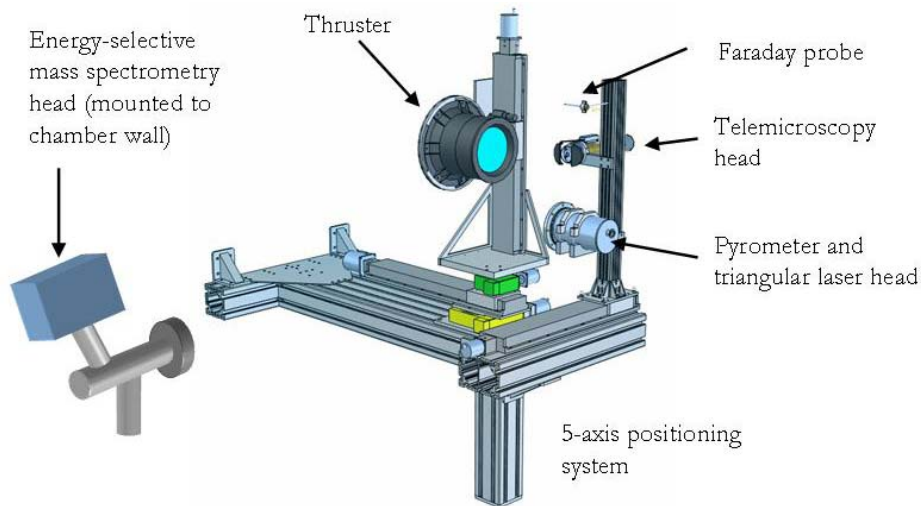


Figure 1: Experimental setup with the 5-axis positioning system and the mounted diagnostic tools [1,2].

More details are given in Ref. [1,2].

B. The Thruster RIT-22

Test object is the gridded ion thruster RIT-22 (Figure 2) by Astrium EADS. RIT-22 is an advanced radio frequency ion propulsion thruster/engine designed to meet the requirements of commercial and scientific missions. The main characteristics are summarized in Table 1. More details are given in Ref. [3].

In this study, the thruster is operated at three power levels: 1.25 kW (main voltage 1250 V/ main current 1000 mA), 2.25 kW (1500 V/1500 mA), and 4 kW (2000 V/ 2000 A). The total operation time for the tests is about 36 h.

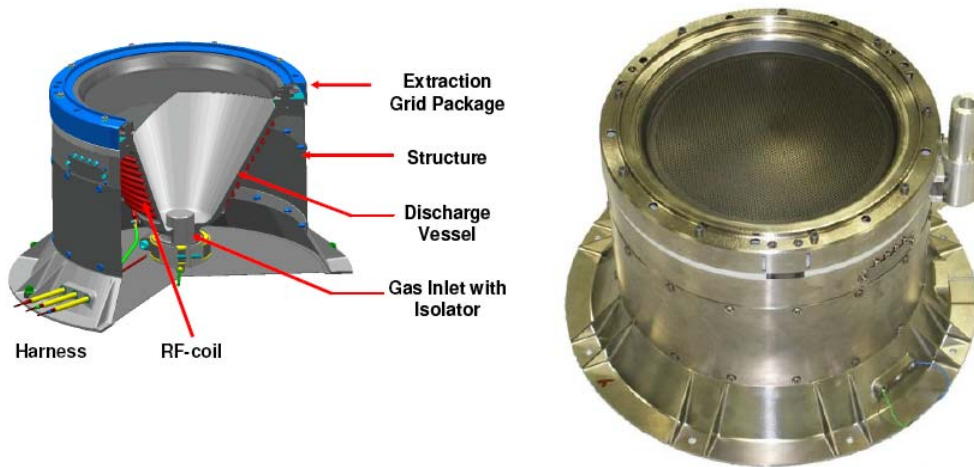


Figure 2: CAD Model of RIT-22 Ion Engine, Middle: RIT-22 EM, SN-01 [3].

Table 1: Main characteristics of the thruster RIT-22.

Characteristic	RIT-22
Propellant:	Xenon
Ionisation principle:	Radio frequency excitation
Discharge chamber diameter:	22 cm
Beam voltage (nom):	900 to 2200 V
Beam current (nom):	750 to 2500 mA
Power (nom):	4.5 kW at 150 mN and 4400 sec. Isp
Thrust level:	75 to 175 mN (nominal) 40 to 250 mN (demonstrated)
Specific impulse:	3000 to 5500 sec. (nominal) 2500 to 6400 sec. (demonstrated)
Design Life	> 26,000 hours
Overall length:	23 cm
Outer Diameter:	30 cm
Mass:	7 kg

C. The Test Facility

The tests are performed in a large vacuum test facility (LVTF) at Aerospazio (length 11.5 m, diameter 3.8 m, volume 120 m³) and medium-size test facility at JLU Giessen (length 6 m, diameter 2.6 m, volume 3 m³) in order to investigate chamber effects. More details are given in Ref. [3], a picture of the facility is shown in Ref. [4].

III. Test Results

D. The Triangular Laser Head Measurements

In Figure 3 a typical TLH scan is shown. The measurement is done in-situ when the thruster is firing. The scan reveals that the line of holes is tilted by $\sim 1.9^\circ$ with respect to the scan line. From the curve the radius of curvature ~ 467 mm can be determined.

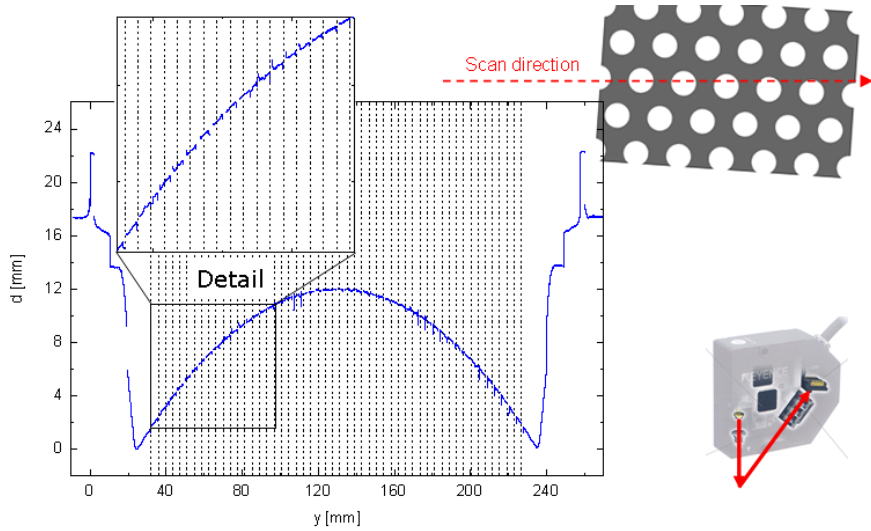


Figure 3: TLH scan across the diameter of the thruster. The vertical dotted lines indicate a line holes with equal spacing. It can be seen that the vertical lines do not always coincide with a hole in the TLH scan, because the line of holes is tilted by about 1.9° with respect to the scan direction, as sketched next to the diagram. Also shown is the TLH setup (<http://www.keyence.com>).

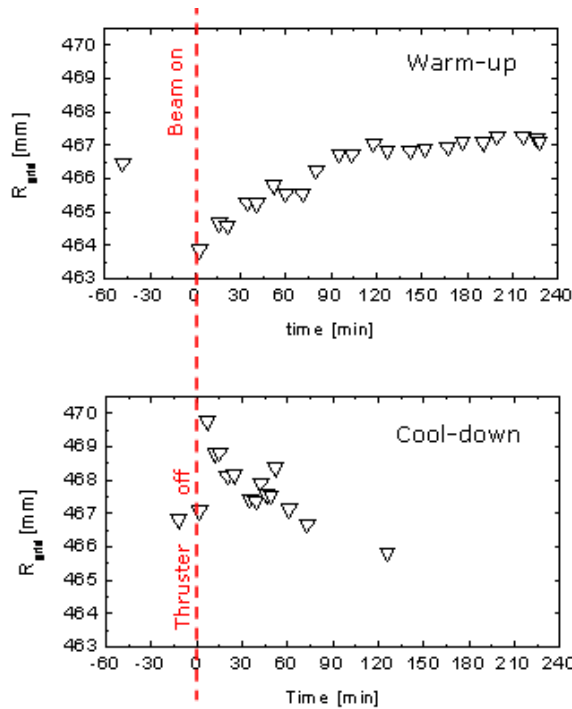


Figure 4: Grid curvature data of the thruster during warm-up (top) and cool-down phase (bottom). The data are obtained by analyzing the TLH scan curves. The thruster is operated at 1.25 kW (1250 V/1000 mA).

Figure 4 shows the variation of the grid curvature after switching on the ion beam and after switching off the thruster. When the beam is switched on, the radius of curvature decreases abruptly, later on it increases and saturates at the value of the cold thruster. When the thruster is switched off, the behavior is contrary; first the radius of curvature increases abruptly and decreases thereafter. However, the variation in curvature itself remains small ($<1\%$).

After switching on it takes about 4 h until the grid curvature gets stable. The same time is need until the thruster gets thermally stable, which can be seen in the grid temperature data (not shown here).

E. The Telemicroscopy System Measurements

In Figure 5 a TMS image of grid holes in the centre of the grid is shown. From the image the grid hole shape, hole diameter, and distances between holes can be determined. The images can be taken with the thruster-off (Figure 5) or with a firing thruster (Figure 6, left image). The determined parameters are comparable. The lateral resolution of the TMS setup is estimated to be about 0.01 mm.

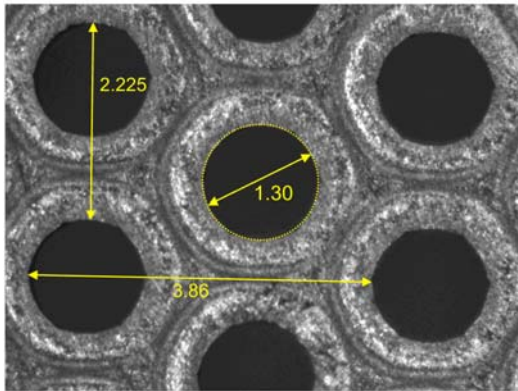


Figure 5: TMS image of the centre hole of the thruster. The hole diameter and the horizontal and vertical distance between neighboring holes are given.

If the thruster is tilted (Figure 6, right image), qualitative information about the hole erosion in depth can be obtained.

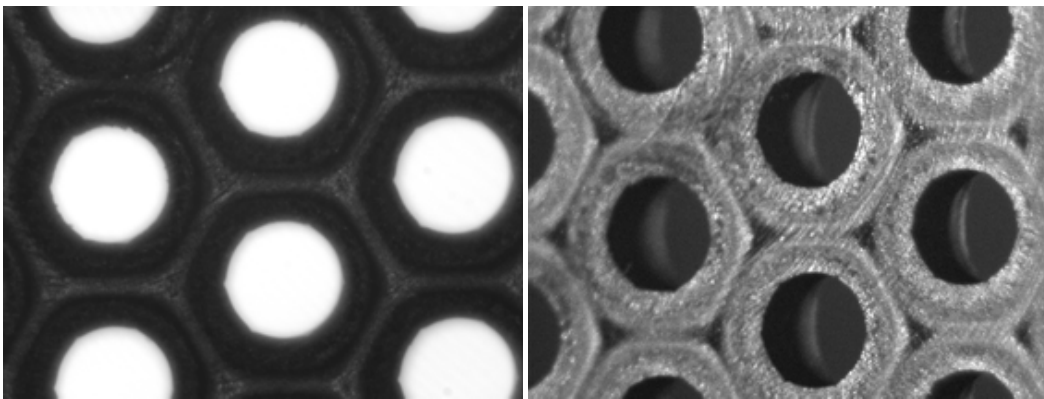


Figure 6: Further TMS images. Left: Centre hole with a firing thruster. Right: Centre hole with a tilted thruster (tilting angle 33°).

F. The Pyrometer Measurements

Pyrometer scan curves across the diameter of the thruster grid are shown in Figure 7. The grid hole area can be easily seen in the graph, it is the interval with the oscillation-like structures. These oscillations are due to the fact that the pyrometer spot always covers both the grid and the grid holes. Depending on the lateral position, the fraction of grid hole area covered by the pyrometer spot changes, i.e. the measured pyrometer scan curve is modulated with a short period. Furthermore, the line of holes is tilted by 1.9° with respect to the scan line, as already shown in the

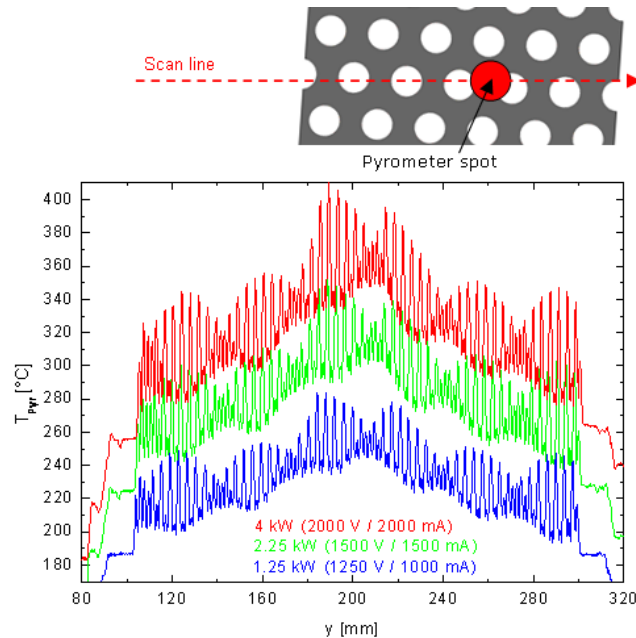


Figure 7: Pyrometer scan curves of a firing thruster at three different power levels. Above the diagram the tilting of the scan curve with respect to a line of grid holes and the size of the pyrometer spot relative to the size of a grid hole is sketched.

TLH scans in Figure 3. Therefore, the pyrometer scan curve is additionally modulated with a longer period.

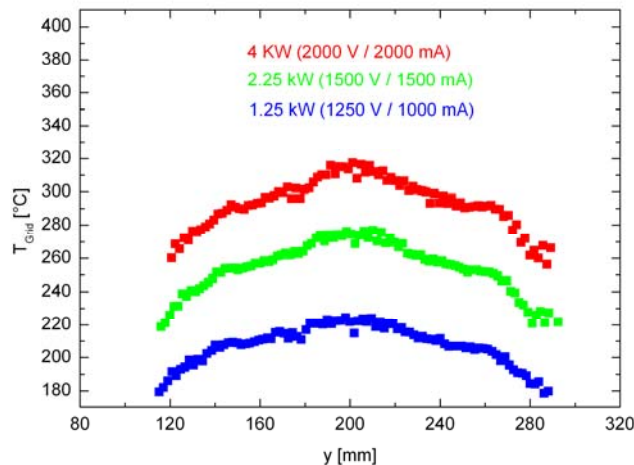


Figure 8: Accelerator grid temperature data of the thruster at different power levels as calculated from the pyrometer scan curves in Figure 7.

The oscillations could not be avoided, but can be used to calculate the grid temperature distribution [5]. First, the area fractions of the pyrometer spot, which covers the grid or the grid hole area is simulated. Then by simple mathematical equations and by comparison of the measured pyrometer scan curve and the calculated area fraction curve, the grid temperature can be calculated [5]. The calculated grid temperatures of the pyrometer scan curves in Figure 7 are plotted in Figure 8. The maximum temperature is in the centre of the grid, which is found approximately 40 K higher than the temperature at the rim. The temperature in the grid centre increases from ~ 220 °C to ~ 320 °C with increasing total power from 1.25 kW to 4.0 kW, respectively.

G. The Faraday Probe Measurements

Current density maps are recorded at distances between 50 mm and 600 mm from the outer accelerator grid using the Faraday probe. The results for three power levels at distances of 100 mm and 600 mm are plotted in Figure 9.

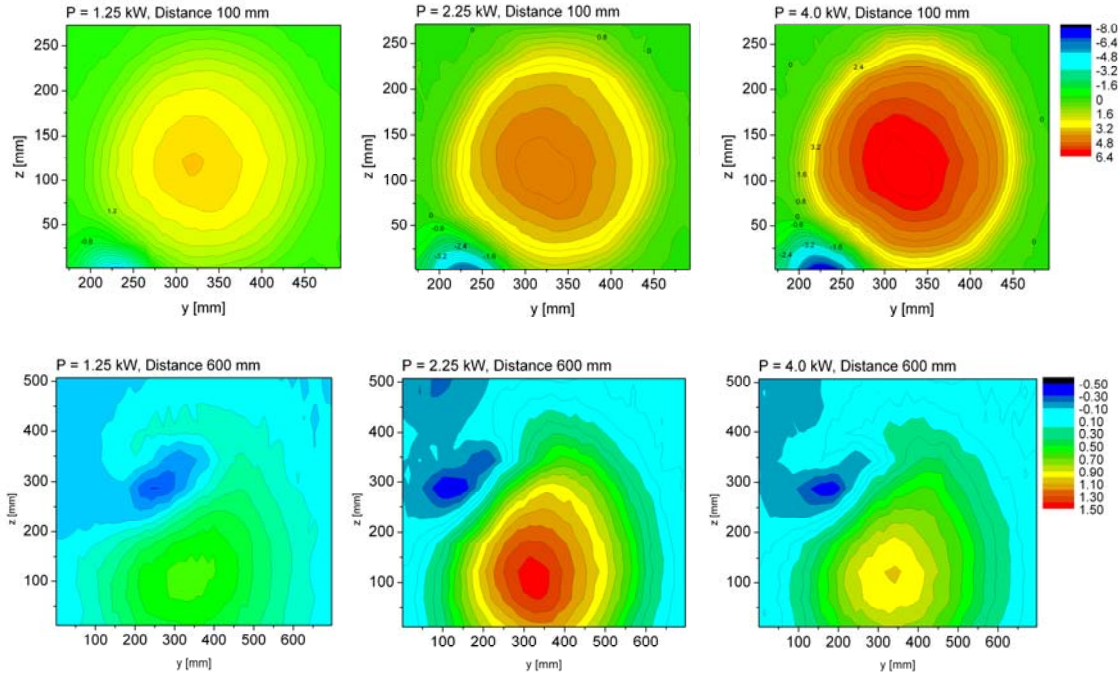


Figure 9: Faraday probe maps measured at distances of 100 mm (top row) and 600 (bottom row) at a power level of 1.25 kW (first column), 2.25 kW, and 4 kW (third row). Note the different lateral scales for the different distances.

At a distance of 100 mm the beam is rotational symmetric with a negative current density spot in the left lower corner. This spot is located at the position of the neutralizer; hence it represents the electrons emitted by the neutralizer. The Faraday probe does not utilize electron suppression; therefore it collects the net sum of ions and electrons. At a distance of 600 mm the negative current density spot is moved to the left upper corner. Again it is the electron beam emitted by the neutralizer, because the spot disappears when the neutralizer is switched off. Othmer [6] performed model calculations which suggest the electron beam oscillates around the ion beam depending on its parameters. Here experimental evidence is presented. Further activities are needed in order to understand this behavior. Our first model calculations suggest that the energy of the electrons is an important parameter. When the energy is high, the electron beam just passes the ion beam. The ion current is still compensated by the electron current, but there is no space charge compensation in the beam. When the energy of the electrons is low, the electrons are more deflected towards the ions and the space charge compensation is improved. For a detailed understanding further investigations are required. Dedicated activities are strongly recommended.

H. The Energy-Selective Mass Spectrometry Measurements

ESMS energy scans at $M^* = 132$ amu at different extraction angles are shown in Figure 10. A mono-energetic energy distribution is found. The intensity drops towards higher extraction angles.

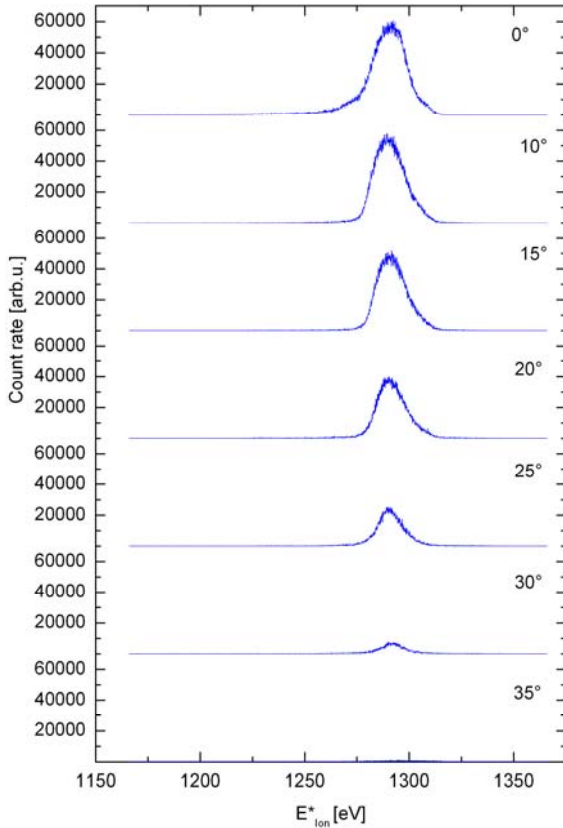


Figure 10: ESMS energy scans ($M^* = 132$ amu) at different angles with respect to the thruster axis. The thruster is operated at 1.25 kW.

In Figure 11 a mass scan at the peak energy is shown. Single charged and a very small fraction of double charged ions can be seen. The signal at the mass of the triple charged ions is below the detection limit. By comparison of the intensities, it is found that the fraction of double charged ions is below 1 %, and of triple (including higher) charged ions below 0.1 %.

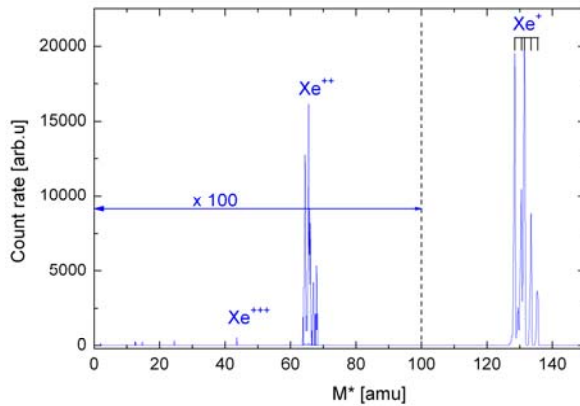


Figure 11: ESMS mass scan ($E^* = 1290$ eV). For $M^* < 100$ amu the curve is multiplied by a factor 100 for clarity. The thruster is operated at 1.25 kW.

IV. Conclusion

We have set up a new, modular diagnostic system for electric propulsion thruster characterization. It is successfully used to characterize in-situ a gridded ion thruster RIT-22, even measurements with a firing thruster are reported. A comprehensive set of parameters is obtained: grid curvature, grid hole diameter, grid hole distances, grid

temperature, current density profiles, energy distribution, mass distribution, and composition of the ion beam. The diagnostic system is not limited to gridded ion thrusters. It can be used for other electric propulsion thruster types too. The new diagnostic system is a powerful platform and we intend to report on more activities in the future.

Acknowledgments

The work was performed in the frame of ESA/ESTEC contract 20461/06/NL/CP "Development of Advanced Electric Propulsion Thruster Characterization Diagnostics". .

References

- [1] C. Bundesmann, M. Tartz, F. Scholze, H.J. Leiter, F. Scortecci, H. Neumann, "An advanced in-situ diagnostic system for characterization of electric propulsion thrusters", Rev. Sci. Instrum., to be submitted..
- [2] C. Bundesmann, M. Tartz, F. Scholze, H. Leiter, D. Feili, H. Neumann, "An advanced characterization system for studying plasma properties, ion beams, and mechanical parts of ion thrusters", Proceedings of 5th International Spacecraft Propulsion Conference (Space Propulsion 2008), Crete, Greece, May 5-8, 2008.
- [3] H.J. Leiter, R. Kukies R. Killinger, E. Bonelli, S. Scaranzin, F. Scortecci, H. Neumann, M. Tartz, "RIT-22 Ion Propulsion System: 5,000h Endurance Test Results and Life Prediction", AIAA 2007-5198.
- [4] C. Bundesmann, M. Tartz, F. Scholze, H. Neumann, F. Scortecci, S. Scaranzin, P.-E. Frigot, J. Gonzalez del Amo, R.Y. Gnizdor, "In-situ temperature, erosion, beam and plasma characterization of a SPT-100D EM1 with an advanced electric propulsion diagnostic system", IEPC-2009-141.
- [5] C. Bundesmann, M. Tartz, F. Scholze, H.J. Leiter, F. Scortecci, H. Neumann, "In-situ measurement of the grid temperature distribution of a gridded ion thruster RIT-22 by pyrometer line scans", Rev. Sci. Instrum., to be submitted..
- [6] C. Othmer, "Numerical simulations of ion thruster-induced plasma dynamics", Dissertation, Universität Braunschweig, Germany, 2001.